Available online at www.sciencedirect.com
SCIENCE DIRECT
Brain Research 963 (2003) 139–149
BRAIN RESEARCH
www.elsevier.com/locate/brainres

Research report

NMDA receptor blockade in intact adult cortex increases trafficking of NR2A subunits into spines, postsynaptic densities, and axon terminals

Chiye Aoki[a,*], Sho Fujisawa[a], Veera Mahadomrongkul[a], Priti J. Shah[a], Karim Nader[b], Alev Erisir[c]

[a]*Center for Neural Science, New York University, Rm 809, 4 Washington Pl., New York, NY 10003, USA*
[b]*Department of Psychology, McGill University, Montreal, Canada*
[c]*Department of Psychology, University of Virginia, 102 Gilmer Hall, PO Box 400400, Charlottesville, VA 22904-4400, USA*

Accepted 28 October 2002

Abstract

Past in vitro studies have used immunofluorescence to show increased clustering of the NR1 subunits of NMDA receptors (NMDAR) following NMDAR blockade, indicating that NMDARs self-regulate trafficking to and from spines. However, since a substantial portion of spinous NMDAR subunits can reside at sites removed from plasma membranes, whether or not these immunofluorescent clusters are synaptic remains to be shown. Also, the NR2A/B subunits undergo activity-dependent switching at synapses, indicating that their subcellular distribution may be regulated differently from the NR1 subunits. We examined the issue of NMDAR autoregulation by determining whether in vivo NMDAR blockade enhances trafficking of the NR2A subunits toward spines and more specifically to postsynaptic densities (PSDs) of already mature synapses. Seven adult rats received unilateral intra-cortical infusion of the NMDAR antagonist, D-AP5 for 1/2–2 h and the inactive enantiomer or the solvent, alone, in the contralateral cortex. Using an electron microscope, ~5600 cortical spines originating from the two hemispheres of the seven adult animals were analyzed for the location of NR2A subunits. In six out of the seven cases analyzed, the D-AP5-treated neuropil exhibited increased immunolabeling at PSDs and a concomitantly great increase at non-synaptic sites within spines. NR2A subunits also increased presynaptically within 1/2 h but not after 1 h. These findings indicate that NR2A subunits in intact, adult cortical neurons are prompted to become trafficked into spines and axon terminals by NMDAR inactivity, yielding an increase of a readily available reserve pool and greater localization at both sides of synapses.

Theme: Neurotransmitters, modulators, transporters, and receptors

Topic: Excitatory amino acids: physiology, Pharmacology and modulation

Keywords: NR2A; NMDA receptor; Activity-dependent; Synaptic plasticity; Trafficking; Ultrastructure; Electron microscopy

1. Introduction

NMDA receptor (NMDAR) activation is a key step linking sensory experience to maturation and strengthening of glutamatergic synapses. Such synaptic changes modify receptive field properties of individual cortical neurons and cortical maps to reflect sensory experiences [23,26]. Synaptic strength is determined by intracellular mechanisms that jointly regulate transmitter release and postsynaptic concentration of receptors [38,48]. Ultimately, knowledge about the mechanisms linking sensory experience to modified cortical circuits will require understanding of the NMDAR activity-dependent trafficking of glutamatergic receptor subunits to and from synapses.

The cellular mechanisms underlying glutamate receptor clustering at synapses have been elucidated using dissociated neonatal neurons. Here, the pharmacological blockade of NMDAR causes a large increase in the density of NR1-immunoreactive fluorescent clusters along dendrites while blockade of AMPA-type receptors (AMPAR) leads to increases of AMPAR subunits without changes in NMDARs [36,37,46]. These clusters are assumed to be synaptic, based on their proximity to the presynaptic marker, synaptophysin. On the other hand, NR1-immuno-

*Corresponding author. Tel.: +1-212-998-3929; fax: +1-212-995-4011.
E-mail address: chiye@cns.nyu.edu (C. Aoki).

0006-8993/02/$ – see front matter
PII: S0006-8993(02)03962-8

reactive fluorescent clusters are observed within dendritic shafts as well, i.e. prior to their trafficking towards axo-spinous excitatory synapses [47], indicating that NR1 subunits can form clusters at non-synaptic sites. Moreover, a possibility remains that some NMDARs are synaptic even if not detectable as immunofluorescent clusters, because they occur at concentrations too low to be detectable.

Thus, while these elegant immunofluorescent studies have allowed for direct visualization of NMDAR activity-dependent NMDAR-trafficking, they also raise interesting new questions. One point is that the clustered fluorescence, presumed to be synaptic, also represents the presence of receptor subunits in spine cytoplasm. These may be reserves that are inserted into synaptic membranes in response to reduced synaptic transmission under a variety of physiological states. This idea is prompted by our previous electron microscopic immunocytochemical studies, in which we noted that the PSD-scaffolding protein, PSD-95, and NR1 subunits occur not only at synapses but also along non-synaptic membranes within spines and dendritic shafts of mature neurons [5,17]. The same and other studies also revealed NMDAR subunits in axon terminals [1–3,12,17] which could participate in activity-dependent regulation of neurotransmitter release [6,8–10,13,20] and axon sprouting [15].

Another question is whether the activity-dependent NMDAR trafficking into spines is a mechanism reserved for neonatal neurons undergoing synaptogenesis, or is also triggered within adult neurons of intact tissue, even though these already possess stable, mature synaptic sites for anchoring NMDAR subunits. This question is particularly pertinent for the NR2A subunits, shown during development to confer adult phenotypes of NMDAR currents in response to experience [34,43].

To address these questions, we employed immuno-gold as a non-diffusible electron microscopic label to localize NR2A subunits of NMDAR precisely at pre-, post- and peri-synaptic sites of intact, mature, cortical neurons. NMDAR activity-dependence was determined by assessing whether NMDAR blockade increases the relative frequency of NR2A-immunopositive synapses.

2. Materials and methods

2.1. Drugs

D-AP5, the NMDAR antagonist, and its inactive enantiomer, L-AP5, were purchased from RBI-Sigma. The concentrations of the drugs were 5 mM, dissolved in sterile saline. The solution was prepared within 2 h prior to application.

Diethyldithiocarbamic acid (DEDTC) was purchased from RBI-Sigma. This drug was administered 15 min prior to sacrifice, while the animal was anesthetized, so as to minimize background immunolabeling arising from silver enhancement of endogenous metals [52].

2.2. Anesthesia

Rats were anesthetized using Nembutal (50 mg, i.p.). Anesthesia was maintained throughout the 30-min to 2-h surgical procedure and the perfusion that followed.

2.3. Drug application

The drug treatment of each animal is summarized in Table 1. All procedures followed a protocol approved by the NYU Animal Care and Use Committee.

For animal #51799, intracortical infusion of D-AP5 was achieved by using a stereotaxic apparatus to position the tip of the Hamilton syringe at the coordinate AP −5.0 mm, ML ±3.0 mm and V 1.7 mm. The volume infused was 400 nl, delivered over 5 min. An identical procedure was followed to deliver the control solution into the contralateral hemisphere. In six subsequent animals, ID Nos. #52699-1, #52699-2, #1, #7, #8 and #9, D-AP5 was applied by placing a piece of gelfoam, ~1 mm×1–3 mm and saturated with the drug, gently over the sensory area of cortex. The area to be superfused in this way was exposed using a dental drill to remove a small portion of the skull, then using a 26-gauge hypodermic needle to pierce the dura mater. Care was taken to avoid nicking blood vessels or touching the cortical surface directly with the needle. Again, the contralateral hemisphere was treated identically, except that the gelfoam piece was saturated with the control solution.

Animals #52699-1 and #52699-2 were treated with D-AP5 for 2- and 1-h, respectively. All others were treated with D-AP5 for 1/2 h before sacrifice by transcardial perfusion with fixatives.

For animals #51799, #52699-1 and #52699-2, the data collection and analyses were performed by an experimenter who was not naïve to the surgical manipulation. For animals #52699-1 and #52699-2, the data collection and analyses were re-run by experimenter naïve to the surgical manipulation. For all subsequent cases, i.e. animals #1, #7, #8, and #9, the hemisphere receiving D-AP5 was randomized and data collection and statistical analyses were performed by an experimenter naïve to the surgical manipulations.

2.4. Tissue preparation

The transcardial perfusion was preceded by i.p. injections of DEDTC (Sigma) at a dose of 1 g/kg, to minimize background labeling arising from silver enhancement of endogenous metals [52]. While still anesthetized, animals were sacrificed by perfusion with a fixative consisting of 4% paraformaldehyde and 1% glutaraldehyde. Following perfusion, the brain was excised, pre-

pared into 3-mm thick coronal blocks using a razor blade, then post-fixed in the same fixative. For each animal, one hemisphere was marked by hole punches, so as to allow identification of the left and right sides of free-floating sections (see below), but randomized with respect to drug treatment, so as to avoid disclosure of the experimental hemisphere to the experimenter performing tissue processing. The 3-mm thick blocks were sectioned using a vibratome set at a thickness of 40 μm. Aldehyde-fixation was terminated within 24 h following perfusion by treating vibratome sections with a reducing agent, sodium borohydride (1%), dissolved in 0.1 M phosphate buffer (pH 7.4). These sections were rinsed repeatedly with 0.1 M phosphate buffer to remove excess sodium borohydride, then stored free-floating for up to 4 months in a buffer consisting of 0.01 M PB (pH 7.4) with 0.9% sodium chloride (saline) and 0.05% sodium azide (PBS-azide), at an ambient temperature of 4 °C.

2.5. Immunocytochemistry

The immunocytochemistry procedure used silver-intensified colloidal gold (SIG) to mark antigenic sites [4,11]. The SIG procedure differs from the most commonly used protocols, in that it was designed to amplify antigen detection by employing gold-conjugated anti-biotin (GAB1 from Ted Pella) to recognize biotinylated secondary antibodies [4]. In brief, six to eight sections from each hemisphere containing the treated zone of the somatosensory cortical area were incubated for 30 min in PBS-azide containing 1% bovine serum albumin (BSA; Sigma) to block background staining. Then, the sections were incubated in the following sequence, always interleaved by rinses: 3 days at 4 °C in PBS-BSA-azide containing 10 μg/ml of rabbit anti-NR2A-antiserum (Upstate); 30 min in biotinylated goat anti-rabbit IgG (Vector), diluted at a concentration of 1:200 using PBS-azide; 3-h in goat anti-biotin conjugated to 1-nm colloidal gold particles (GAB1, Ted Pella), diluted to 1:200 using PBS-BSA, without azide; 10 min in PBS containing 2% glutaraldehyde to cross-link antibodies to antigenic sites; 1 min in 0.1 M citrate buffer (pH 7.4); 12 min in a silver-intensification solution, at room temperature (Amersham). The silver-intensification step was terminated by rinsing sections with the citrate buffer. The sections were processed osmium-free, using Phend's published procedure [41], also detailed in Aoki et al. [4], so as to minimize loss of silver-intensified gold particles by oxidation. This osmium-free procedure uses tannic acid, iridium tetrabromide, and uranyl acetate to preserve membrane and cytoskeletal ultrastructure. After embedding these vibratome sections in resin (Embed 812), ultrathin sections from the surfaces of vibratome sections were prepared at a thickness of 85 nm. The ultrathin sections were further counterstained for 10–30 s using Reynold's lead citrate and examined using a JEOL 1200XL electron microscope.

2.6. Data analysis

2.6.1. Sampling area

The area for quantitative analysis was judged to be suitable for sampling at a magnification less than 3000×. At this magnification, identification of the layer 1/layer 2 boundary was possible, using the appearance of pyramidal neuron somata in layer 2 as the indicator. The surface-most portions of 40-μm vibratome sections also could be visualized by the abrupt transition between neuropil and embedding matrix. An example of such transitions can be seen in Fig. 1 (panels A and B, left). Neuropil regions exhibiting metabolic stress were detectable, based on dendritic shafts that were swollen and vacuous. Such portions of the neuropil were not included in the analysis. At the magnification of 3000×, individual synapses were not detectable. This was an important aspect of the procedure for selecting areas to sample, particularly for the cases that were not performed blind, because this step assured against biased selection of neuropil regions differing in density of spinous or axonal labeling prior to performing statistical analyses.

The one animal, #51799, that received AP5 infusion by the Hamilton syringe, showed metabolic stress within a distance of 0.2 mm from the cannula shaft and traversing throughout the depth of cortex. This region was avoided in sampling. Thus, sampling was performed within a range of 0.2 μm–2 mm from the infusion site of both experimental and control hemispheres. For gelfoam-treated hemispheres, identification of layer 1 was important, because this region was expected to have received maximal exposure to the drugs. In general, ultrastructure changes reflecting metabolic stress was less for the gelfoam-treated hemispheres. For this reason, drug application using gelfoam was favored over the Hamilton syringe. For all cases, portions of the neuropil containing less than ten silver-intensified gold particles (SIGs) per 5 μm^2 were not included in the analysis.

The areal density of spines was estimated for each case, so as to ascertain whether the drug treatment might have induced tissue swelling, shrinkage, spinogenesis or spine pruning. Spine density varied between animals and between hemispheres, but these differences were insignificant and not correlated with drug treatments or NR2A immunolabeling.

2.6.2. Sampling procedure

Once a suitable area was chosen, usually contained within a square of 400-mesh thin bars of grids (55 μm×55 μm=3025 μm^2), systematic sweeps were performed to collect non-overlapping electron microscopic images at final magnifications ranging from 30,000 to 100,000×. These magnifications permitted visualization of an area that was at least 6 μm^2 and resolution of the presynaptic versus postsynaptic membranes. The initial phase of analyses was done on-line, i.e. while looking on the

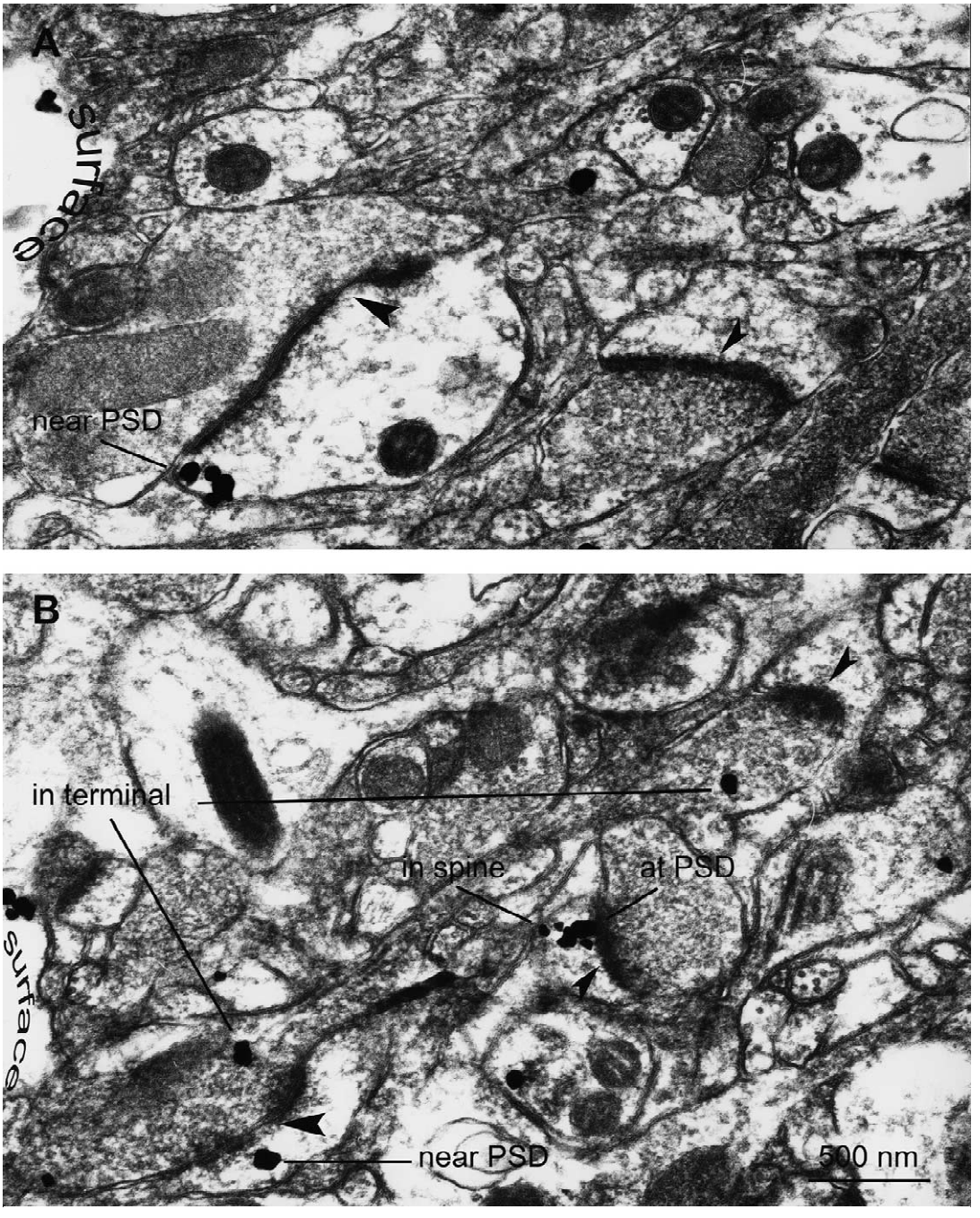

Fig. 1. Electron micrographs showing NR2A SIG immunolabeling within intact, adult cerebral cortex. The electron micrographs show examples of NR2A immunolabeling by the SIG procedure at synaptic and peri-synaptic sites. Some of the synapses occurring within the field are labeled by arrowheads that point to postsynaptic densities (PSD). The neuropil was sampled strictly from the surface of vibratome sections, where the borders between brain tissue and tissue-free, resin-only zone are evident (to the lower left, in both panels). SIG labeling, generated by the pre-embed procedure, is most abundant within such zones. In panel A, a cluster of SIG particles occurs near the postsynaptic density (PSD). In the center of panel B, a spine forming a synapse with a terminal shows NR2A labeling directly at the PSD. The same spine also shows SIG particles that are neither near nor at PSDs ('in spine'). Additional SIG particles occur near but not at the PSD. The spine to the lower left shows an SIG particle near but not directly over the perforated PSD. The same field shows two presynaptic axon terminals with SIG particles within.

electron microscope. The subsequent analyses were done off-line, by first capturing the images either photographically or using a CCD camera (AMT, MA).

2.6.3. Identification of synapses, presynaptic axon terminals and spines

Since NMDARs subserve excitatory synapses, and these

are exclusively asymmetric within adult cortex [2], the localization of NR2A subunits was analyzed in relation to asymmetric synapses on spines. Asymmetric axo-spinous synapses were identified using the following criteria [14]: (i) presence of synaptic vesicles (at least one) adjacent to a plasma membrane, and at least three more vesicles within the same profile, allowing identification of the profile as a presynaptic terminal; (ii) parallel alignment of the spine plasma membranes with that of the terminal; (iii) presence of the electron-dense postsynaptic density (PSD) opposing the terminal. Clear visualization of synaptic cleft was not considered a necessary criterion.

2.6.4. Categorization of SIG labels

Each encountered axo-spinous synaptic junction was given an ordinal number, and the sites of SIG particles occurring in their vicinity were categorized as one or more of the following: within the cytoplasm of a presynaptic terminal but not near or at presynaptic membrane; near the presynaptic membrane; precisely at presynaptic membrane; precisely at PSDs within spine; near but not at PSDs within spine (near PSDs), and within spine but not near or at PSDs. SIG particles were considered to reflect labeling 'at' PSDs or synaptic plasma membranes when SIG particles were found directly overlying these organelles (Fig. 1B). SIG particles were considered to reflect labeling 'near' PSDs or synaptic membranes when they did not touch the organelles but were within a distance equal to the thickness of PSDs. Examples of this category are shown in Fig. 1A,B. Those categorized under the most inclusive category, 'anywhere within spines' (Table 1) or 'anywhere within axon terminals' (see Fig. 1B for an example) were SIG particles that occurred within the membrane-delimited cytoplasm of spines or terminals and included those that were not 'near' or 'at' pre- or postsynaptic plasma membranes.

2.7. Statistical analysis and quantification

We wanted to determine whether the NR2A-immunolabeling or the drug effect was homogeneous over the area sampled. This question was particularly important during the initial phase of the study, since the depth of penetration of the drug from the infusion site was not known. Starting from the region closest to the drug-infusion site but still clearly out of the metabolically stressed region, we monitored for potential changes in immunolabeling. Rather than combining data arising from a large neuropil area, a series of smaller neuropil areas, each containing 30–33 axo-spinous synaptic junctions, were quantitatively assessed for SIG labeling. The 30–33 axo-spinous synaptic junctions encountered within small sampled areas will be referred to as 'groups'. Labeling in spines and the presynaptic terminals were tallied for every group. The number of synapses per group was 33 for cases #51799, #52699-1 and #52699-2, and was 30 for the subsequent cases. This tallying within groups was repeated at least five times (for animal #51799) and at most 30 times (#52699-1). Outcome of this analysis indicated that, for the gelfoam-treated cases, the drug effect was not detectably varying within layer 1 and a 1-mm radius from the infusion site. Similarly, for the case that received the drug via a Hamilton syringe, NR2A labeling was not detectably varying within the range 200–750 μm from the vertically oriented injection path. Once this pattern was ascertained, analysis of neuropil from later cases (animals #1, #7, #8, and #9) and the re-analysis of neuropil from animals #52699-1 and #52699-2, were standardized to ten groups per hemisphere and the group was standardized to 30 axo-spinous synaptic junctions (i.e. 300 axo-spinous synaptic junctions from the experimental hemisphere E in Tables 1 and 2 and 300 more axo-spinous synaptic junctions from the contralateral, control hemisphere (C in Tables 1 and 2). The mean and S.E.M. values of labeled axo-spinous synaptic junctions per group were derived for each hemisphere, using this procedure.

The working hypothesis of the study was that NMDAR blockade up-regulates net influx of NMDAR subunits towards synapses. Our prediction was that NR2A-immunolabeling of synapses would be greater following a 30-min NMDAR-blockade by the antagonist, D-AP5, compared to control conditions, in which NMDAR activation is allowed to occur at a basal level. The directional nature of this hypothesis led us to adopt a one-tailed (unpaired) *t*-test in which we made allowances for unequal group variances. We evaluated all *P*-values against an α level of 0.05.

3. Results

3.1. Light microscopy reveals robust NR2A immunoreactivity in both experimental and control hemispheres

Somata and apical dendrites were labeled for NR2A throughout the layers of the sensory cortex. The distribution of NR2A immunoreactivity detectable by the SIG procedure resembled the cortical distribution pattern reported earlier for NR2A by peroxidase-based methods [39], indicating successful silver-intensification of 1-nm colloidal gold labels. The portion of layer 1 immediately underlying the duratomy exhibited blood clots and dense acellular aggregates of SIG particles indicative of high background labeling. These regions were not subjected to ultrastructural analyses. Instead, blocks for ultramicrotomy were designed to include portions of layer 1 within the primary sensory cortex that were adjacent to but clearly non-overlapping with these darkened portions. At the light microscopic level, inter-hemispheric differences in immunolabeling were not apparent, thus allowing EM sam-

pling to proceed without knowledge of the surgical manipulation.

3.2. Electron microscopic visualization of the neuropil shows no correlation between spine density and drug treatment

Immunolabeled spines and presynaptic terminals were tallied for each group of 30–33 axo-spinous synaptic junctions encountered, following systematic sweeps of ultrathin sections exhibiting tissue–resin interface. For both the control and D-AP5-treated neuropil, the areal density of synapses varied by ~50% above and below the mean, without any pattern that varied consistently across drug treatments. For this reason, the labeling was not normalized to the area surveyed, but rather, to a set number of axo-spinous junctions encountered (30 or 33).

By electron microscopy, the positions of SIG labels relative to synaptic junctions could be resolved with ease at a magnification of 12,000× and higher. Moreover, several distinct clusters of SIG could be resolved within single spines. SIGs were not confined to PSDs or even within spines, but were also present in axon terminals and spines (Fig. 1B).

3.3. Postsynaptic labeling for NR2A is greater within D-AP5-treated neuropil

The number of spines exhibiting SIG particles precisely over PSDs varied across the control hemispheres (Table 1). However, within-animal, inter-hemispheric differences were greater than this: six out of seven animals exhibited greater than two-fold increase of labeling at PSDs within the experimental (E) hemispheres that received D-AP5 infusion ($P<0.05$, unpaired t-test). Within the cortex of animal #51799, which received D-AP5 via a Hamilton syringe, augmentation of NR2A-labeling was evident within a column of tissue at a distance less than 750 μm from the infusion site (columns labeled 'E-nr' in Table 1). At a distance greater than 750 μm from the infusion site (E-far in Table 1), the neuropil labeling was not significantly different from the values obtained in the contralateral, control hemisphere near injection of solvent, alone (C-Nr in Table 1).

In Table 1, the values are means±S.E.M. of the number of immunolabeled spines encountered per group of axo-spinous synaptic junctions. For animals #51799, #52699-1 and #52699-2, each group contained 33 axo-spinous synaptic junctions. For animals #1, #7, #8 and #9, each

Table 1
NR2A immunolabeling within spines forming axo-spinous synaptic junctions

Animal ID	AP5 duration (h)	Spines labeled at PSDs		Spines labeled at or near PSDs		Spines labeled anywhere within	
		E	C	E	C	E	C
#51799 (891 spines) E=right	1/2	**E-nr 2.2±0.6*** E-far 0.8±0.4	C-Nr 1.0±0.3	**E-nr 3.0±0.6*** E-far 0.9±0.4	C-nr 1.0±0.3	**E-nr 4.0±0.7*** E-far 2.1±0.6	C-nr 1.0±0.3
#52699-1 (1584 spines) E=left	2	**1.4±0.3***	0.1±0.6	**2.3±0.45***	0.3±0.1	**3.9±0.8***	1.5±0.3
52699-2 (792 spines) E=left	1	**5.2±0.5***	2.7±0.7	**9.4±0.7***	6.3±1.4	**13.4±1.0***	8.7±0.9
#1 (600 spines) E=right	1/2	0.8±0.3	0.7±0.25	1.8±0.4	2.3±0.3	3.0±0.5	4.2±0.6
#7 (600 spines) E=left	1/2	**0.5±0.2***	0±0	**1.7±0.5***	0.6±0.3	**3.9±0.8***	2.1±0.7
#8 (600 spines) E=right	1/2	**4.7±1.1***	1.8±0.5	**7.7±1.5***	3.7±0.5	**9.4±1.8***	6.5±0.7
#9 (600 spines) E=left	1/2	**4.4±0.5***	2.4±0.45	**10.2±0.7***	5.1±0.7	**13.7±0.54***	8.7±0.7

The values are means±S.E.M.s of the number of immunolabeled spines encountered within an area of neuropil per group-unit of synapses (group-unit=33 synapses for animals #51799, #51699-1 and #51699-2; group-unit=30 synapses for animals #1, #7, #8 and #9). E indicates mean and S.E.M. of immunolabeling obtained from the experimental neuropil; C indicates corresponding values obtained from the control neuropil. E-nr and E-far indicate values obtained from neuropil near and far from the injection site of D-AP5; C-nr and C-far indicate values obtained from the neuropil near and far from the injection site of the solvent in the contralateral hemisphere. The total number of spines (labeled and unlabeled) encountered from both hemispheres of each case are indicated in parentheses under the column 'Animal ID'. Bolded numbers and the asterisks indicate that the means for the experimental neuropil, shown under columns 'E' were statistically different by a one-tailed (unpaired) t-test. All P-values were evaluated against an α level of 0.05.

group contained 30 axo-spinous synaptic junctions. The number of groups per hemisphere varied from five to 30. E indicates mean and S.E.M. of immunolabeling obtained from the experimental neuropil; C indicates corresponding values obtained from the control neuropil. E-nr and E-far indicate values obtained from neuropil near and far from the injection site of D-AP5; C-nr and C-far indicate values obtained from the neuropil near and far from the injection site of the solvent in the contralateral hemisphere. The total number of spines forming axo-spinous synaptic junctions (labeled and unlabeled) encountered from both hemispheres of each case are indicated in parentheses under the column 'Animal ID'. The experimental hemisphere is indicated as 'left' or 'right'.

Bolded numbers and the asterisks indicate that the means for the experimental neuropil, shown under columns 'E' were statistically different by a one-tailed (unpaired) *t*-test. All *P*-values were evaluated against an α level of 0.05.

Inter-hemispheric differences in synaptic labeling by SIGs were detectable in the same six cases, even after expanding the categorization of synaptic labeling to include those with SIG labeling near but not precisely over PSDs. These spines exhibited SIG particles at positions within 25 nm from the edge of PSDs, or a distant equivalent to the width of one PSD (column labeled 'Spines labeled at or near PSDs', in Table 1). For these animals, labeling within experimental hemispheres was still evident under the third criterion, designed to match those of published studies that used immunofluorescence for detection: namely, labeling at, near or far from PSDs but still within spines. In Table 1, the values are shown under the column, 'Spines labeled anywhere within'. The increases in labeled spines were accompanied by increases in the number of SIG particles per spine (not shown).

More SIG particles occurred at sites away from PSDs than strictly near or at PSDs. Similarly, twice as many spines showed SIGs at sites away from PSDs, compared to those spines with SIGs precisely at PSDs (compare the values 'Spines labeled anywhere within' to the values 'Spines labeled at PSDs' within Table 1). This difference in labeling between PSDs and the intracellular matrix of spines indicates that a large number of NR2A subunits occur as part of a reserve pool, and this non-junctional pool of NR2A subunits is responsive to NMDAR-blockade.

Of the seven cases, animal #1 was the exception. The two hemispheres exhibited no difference in the number of labeled synapses, labeled spines or SIGs within spines (Table 1).

3.4. Presynaptic labeling for NR2A is enhanced by D-AP5 treatment

The initial observations indicated that NR2A immunolabeling occurs within axon terminals as well as spines [2]. We sought to determine whether the presynaptic pool of NR2A subunits might also be regulated by NMDAR activity. Thus, the last four cases that underwent quantitative analyses (animals #1, #7, #8 and #9) were subjected to tests to determine whether D-AP5 treatment correlated with elevation of NR2A immunoreactivity within presynaptic axon terminals.

The results revealed that all four cases showed increases in synapses with presynaptic labeling (Table 2, right-most column), although the increase was not statistically significant for animal #9 ($P=0.07$). This increase of synapses with presynaptic labeling was accompanied by increases in the number of SIG particles within axonal cytoplasm. However, of the four cases, only two reached statistical significance in the differences (animals #1 and #8). Interestingly, increased labeling at or near presynaptic membranes occurred even for the case that did not exhibit postsynaptic elevation (animal #1).

The table shows mean and S.E.M. of the number of presynaptic axon terminals and of the number of SIG particles within these terminals per group of axo-spinous synaptic junctions. Each group contained 30 synapses. The number of groups per animal was ten per hemisphere. See the legend to Table 1 for further explanations.

The analysis of presynaptic axon terminal labeling was extended to animals #52699-1 and #52699-2, which received longer D-AP5 treatments. These animals exhibited no inter-hemispheric differences in presynaptic membrane labeling or SIG particles within axon terminals (Table 2).

4. Discussion

4.1. Methodological considerations

To our knowledge, our study is the first to directly examine the effect of NMDAR blockade upon the ultrastructural distribution of NMDAR subunits within intact adult cortex. This assessment was made using a non-diffusible, electron-dense marker, colloidal gold, to maximize precision in NR2A localization. The colloidal gold particles were applied in parallel to the two hemispheric sides of vibratome sections, still connected to one another by fibers of the corpus callosum, prior to embedding in resins required for electron microscopy. The pre-embedding procedure minimized loss of antigenicity as well as inter-hemispheric differences in the immunocytochemical procedure. These advantages allowed for easier isolation of drug effects. The size of colloidal gold was small (1 nm), so as to optimize penetration of the label into fine processes. Subsequent to the formation of antibody-antigen complex containing 1-nm colloidal gold particles, the 1-nm particles were enlarged by silver-intensification (SIG) to facilitate immunodetection.

With this SIG method, we detected NR2A immunoreactivity in ~10% of the spines forming morphologically

Table 2
NR2A immunolabeling in presynaptic axon terminals

Animal ID	AP5 treatment duration (h)	SIGs in terminals		Synapses labeled near presynaptic membrane	
		E	C	E	C
52699-1 (600 terminals) E=left	2	14.5±3.1	14.2±2.3	2.1±0.4	2.1±0.3
52699-2 (600 terminals) E=left	1	14.1±5.7	25.1±5.7	1.0±0.4	1.3±0.5
#1 (600 terminals) E=right	1/2	**6.8±1.9***	0.7±0.4	**1.5±0.4***	0.4±0.2
#7 (600 terminals) E=left	1/2	**2.2±1.3**	0.8±0.8	**0.4±0.2***	0.1±0.1
#8 (600 terminals) E=right	1/2	**19.3±4.4***	1.5±0.6	**6.1±1.5***	0.6±0.3
#9 (600 terminals) E=left	1/2	6±1.9	4.9±1.9	1.8±0.4 $P=0.07$	1±0.3

The table shows mean and S.E.M. of SIG particles within axon terminals and of presynaptically labeled synapses per unit-group of synapses. The unit-groups were 30 synapses for both hemispheres in all cases. See the legend to Table 1 for further explanations.

identifiable, asymmetric synapses. Although this value must reflect some detection failures, the *degree* of failure is difficult to assess, since the number of spines remaining silent cannot be known physiologically and anatomical findings of the past have had constraints similar to ours [2,17,22,24,39]. Post-embed gold (PEG) results indicate that approximately three-fourths of synapses express NR1 subunits [24,40] and a similar proportion contains NR2A and/or NR2B subunits [40] (Fujisawa and Aoki, unpublished observations). As for the NR2A subunits, specifically, no data other than ours are available. Comparisons of the above values suggest that a large fraction of NR2A-negative synapses may be endowed with NR1/NR2B heteromers and, thus, participate in synaptic transmission.

We sometimes encountered difficulty categorizing the SIG labeling as being 'precisely at' versus 'near' PSDs. Despite this ambiguity, the outcomes were consistent across animals and across the tallying performed by three observers, indicating that such variabilities were sufficiently small, allowing for detection of patterns related to the drug treatment. The drug treatment yielded strong effects, in that some produced several-fold increases in NR2A-immunoreactivity, and the smallest increases were doubling.

We do not know why one out of the seven animals did not exhibit a rise in postsynaptic labeling (animal #1). However, the same animal exhibited an increase in axon terminal labeling for NR2A within the hemisphere receiving the NMDAR blocker, as was observed for three other cases analyzed for presynaptic labeling following a 1/2-h treatment. This finding indicates that animal #1, together with all others, received an effective dose of the blocker within the analyzed neuropil. There may be inter-animal differences in the amplitude, rate and subcellular sites for response to NMDAR blockade or zinc chelation by DEDTC.

4.2. Increase of spines immunoreactive for NR2A subunits

Earlier studies had examined trafficking of NR1 subunits following NMDAR blockade within cultured neurons. Our procedure differed from that of earlier studies in several other important ways: (i) we examined adult neurons, while previous studies analyzed neonatal neurons; (ii) we examined neurons still embedded within intact cortical circuits, while previous studies examined dissociated neurons in cultures; (iii) we were able to resolve membranous, cytoplasmic and synaptic localizations by EM, while the earlier ones could not, due to limitation of immunofluorescence; (iv) earlier studies applied pharmacological blockade for longer periods (as long as 40 days), while ours ranged from 1/2 to 2 h; (v) we examined NR2As, while previous studies examined NR1s. Despite of these differences, we are in agreement with the earlier immunofluorescent findings, namely that NMDAR blockade increases the net flux of NMDAR subunits towards spines.

Our findings provide the first demonstration that labeling

specifically at PSDs is elevated by NMDAR blockade. An unexpected and thus more interesting finding is that NR2As predominate at non-synaptic portions of spines. These may serve as the reserve pool. Such non-synaptic pools of the NMDAR subunits also are negatively controlled by NMDAR activation, indicating that an intracellular, diffusible messenger arising from activation of synaptic NMDARs may mediate regulation of non-synaptic NMDARs.

Our previous view had been that activation of synaptic NMDARs might be linked to trafficking of non-membranous NMDAR subunits within spines, because dendritic spines are regarded as independent functional units of neuronal integration [33,49,55,56] and contain PSD-proteins that bind NMDAR subunits [5,18,27,50]. We surmised that trafficking of subunits within spines could be regulated more directly by a rise in intracellular Ca^{2+}, confined to spines following NMDAR activation. However, if the NMDAR-dependent regulation of NMDAR subunit trafficking were confined to the spine cytoplasm, one would have observed a decline of NR2A subunits within the spines' non-synaptic pool, accompanying a rise at or near PSDs. Instead, we observed a net rise both within spine cytoplasm and at PSDs. This finding suggests that NMDAR blockade may be linked to trafficking of NMDAR subunits arising from shafts. Since shafts contain ribosomes and mRNAs [51], trafficking that originates from shafts may accompany de novo synthesis of NR2A subunits. Moreover, proteins required for protein synthesis have also been detected in spines [42]. Thus, if NR2A subunit-mRNAs occur within spines, then spines may also become recruited in the de novo synthesis of NR2A subunits following NMDAR blockade, independently of synthesis and trafficking from dendritic shafts. In support of these views, increases in NR2A protein levels within homogenates have been reported as early as 20 min following LTP-inducing tetani [53].

Even prior to de novo synthesis, there may be NR2A subunits on reserve within dendritic shafts that can be trafficked into spines. Earlier studies [5,7] have detected NMDAR subunits as well as members of the MAGUK family of PDZ domain-containing proteins within dendritic shafts. These members of the MAGUK family of proteins are able to link NR2A subunits with the microtubule machinery residing in dendritic shafts (and not in spines) [7,18,35,50]. Perhaps NMDAR activity-dependent trafficking of NR2A subunits into spines involves mobilization of a reserve pool that is reversibly tethered by members of the MAGUK family of proteins within shafts.

We detected no consistent change in spine density following drug treatment. This was somewhat contrary to expectation, since earlier studies had shown both increases [16,19,29,57] and decreases [21,44,45] in spine density following pharmacological blockade of glutamate receptors. On the other hand, previous studies had used in vitro systems, which may differ from our in vivo states, and there is at least one report of a subtle to no effect, or both an increase and decrease in synapses [30]. Even if pruning or addition of spines took place in response to NMDAR blockade in vivo, this process was apparently not selective for or against the NR2A-containing spines and insufficient to explain the observed increases in NR2A-immunoreactive spines.

While the pharmacological blockade of NMDAR is far from physiological, what this finding suggests is that smaller and more transient decreases in synaptic transmission that occur during normal physiological states may trigger net influxes of NMDAR subunits from shafts to spines. Conversely, increases in synaptic transmission may trigger net effluxes of NMDAR subunits out of spines.

4.3. Increases of presynaptic labeling following NMDAR blockade

The presence of axonal labeling for NR2A subunits is not surprising, in light of past observations of presynaptic labeling for members of the MAGUK family [5], NR1 subunits [2,12,17] and NR2 subunits [12,54]. However, to our knowledge, the present observation is the first to report on an increase of presynaptic NMDAR subunits in response to NMDAR blockade. Assuming that these can form functional receptors, such an increase in the presynaptic expression of the NR2A subunits will allow for increased basal presynaptic Ca^{2+} concentration (i.e. independent of action potentials) which, in turn, can enhance evoked release of transmitters from axons [9,13,28]. Thus, a feedback mechanism can boost synapses that have undergone transient or long-term decreases in excitatory synaptic transmission. Interestingly, the timing of this presynaptic response is slightly different from the postsynaptic one. Moreover, only two of the six animals analyzed show concerted increases both pre- and postsynaptically. These differences suggest that the mechanisms regulating the trafficking of NR2A subunits on the two sides of synapses are likely to be different. One possible difference is that the presynaptic mechanism may or may not involve de novo synthesis of NR2A subunits from local (within terminal) sources. Ribosomes have not yet been visualized in axon terminals [51], but mRNAs for the enzyme, tyrosine hydroxylase, have been detected [31]. Whether or not NR2A-mRNA also occur in terminals has yet to be determined. On the other hand, increased trafficking from preterminal portions of axons or from somata may be possible, particularly since certain members of the MAGUK family are reported to be enriched in axons [5,25,27,32].

Findings of the present study indicate that activity-dependent binding of NR2A subunits with proteins of the MAGUK family and their trafficking together or separately within axons and dendrites would be fruitful topics for future studies.

Acknowledgements

We thank Anita Disney and Robert Levy for their critical reading of the manuscript. This research was supported by R01-EY13145 and R01-NS 41091 to C.A., R01-EY12138 to A.E., the NEI Core Grant (1 P30 EY13079, PI-JA Movshon) and the Office of Naval Research Grant (BAA 99-019, PI-P Lennie).

References

[1] C. Aoki, Postnatal changes in the laminar and subcellular distribution of NMDA-R1 subunits in the cat visual cortex as revealed by immunoelectron microscopy, Brain Res. 98 (1997) 41–59.
[2] C. Aoki, C. Venkatesan, C.-G. Go, J.A. Mong, T.M. Dawson, Cellular and subcellular localization of NMDA-R1 subunit immunoreactivity in the visual cortex of adult and neonatal rats, J. Neurosci. 14 (1994) 5202–5222.
[3] C. Aoki, J. Rhee, M. Lubin, T.M. Dawson, NMDA-R1 subunit of the cerebral cortex co-localizes with neuronal NOS at pre- and postsynaptic sites and spines, Brain Res. 750 (1997) 25–40.
[4] C. Aoki, S. Rodrigues, H. Kurose, Use of electron microscopy in the detection of adrenergic receptors, Methods Mol. Biol. 126 (2000) 535–563.
[5] C. Aoki, I. Miko, H. Oviedo, T. Mikeladze-Dvall, L. Alexandre, N. Sweeney, D.S. Bredt, Electron microscopic immunocytochemical detection of PSD-95, PSD-93, SAP-102 and SAP-97 at postsynaptic, presynaptic and non-synaptic sites of adult and neonatal rat visual cortex, Synapse 40 (2001) 239–257.
[6] N. Berretta, R.S.G. Jones, Tonic facilitation of glutamate release by presynaptic *N*-methyl-D-aspartate autoreceptors in the entorhinal cortex, Neuroscience 75 (1996) 339–344.
[7] J.E. Brenman, J.R. Topinka, E.C. Cooper, A.W. McGee, J. Rosen, T. Milroy, H.J. Ralston, D.S. Bredt, Localization of postsynaptic density-93 to dendritic microtubules and interaction with microtubule-associated protein 1A, J. Neurosci. 18 (1998) 8805–8813.
[8] A.L. Breukel, E. Besselsen, F.H. Lopes Da Silva, W.E. Ghijsen, A presynaptic NMDA autoreceptor in rat hippocampus modulating amino acid release from a cytoplasmic pool, Eur. J. Neurosci. 10 (1998) 106–114.
[9] G. Bustos, J. Abarca, M.I. Forray, K. Bysling, C.W. Bradberry, R.H. Roth, Regulation of excitatory amino acid release by *N*-methyl-D-aspartate receptors in rat striatum: in vivo microdialysis studies, Brain Res. 585 (1992) 105–115.
[10] M. Casado, S. Dieudonne, P. Ascher, Presynaptic NMDA receptors at parallel fiber-Purkinje cell synapse, Proc. Natl. Acad. Sci. USA 97 (2000) 11593–11597.
[11] J. Chan, C. Aoki, V.M. Pickel, Optimization of differential immunogold-silver and peroxidase labeling with maintenance of ultrastructure in brain sections before plastic embedding, J. Neurosci. Methods 33 (1990) 113–127.
[12] J.P. Charton, M. Herkert, C.-M. Becker, H. Schroder, Cellular and subcellular distribution of the 2B-subunit of the NMDA receptor in the adult rat telencephalon, Brain Res. 816 (1999) 609–617.
[13] A.J. Cochilla, S. Alford, NMDA receptor-mediated control of presynaptic calcium and neurotransmitter release, J. Neurosci. 19 (1999) 193–205.
[14] M. Colonnier, C. Beaulieu, An empirical assessment of stereological formulae applied to the counting of synaptic disks in the cerebral cortex, J. Comp. Neurol. 231 (1985) 175–179.
[15] M. Constantine-Paton, H.T. Cline, LTP and activity-dependent synaptogenesis: the more alike they are, the more different they become, Curr. Opin. Neurobiol. 8 (1998) 139–148.
[16] K.S. Cramer, M. Sur, Activity-dependent remodeling of connections in the mammalian visual system, Curr. Opin. Neurobiol. 5 (1995) 106–111.
[17] S. DeBiasi, A. Minelli, M. Melone, F. Conti, Presynaptic NMDA receptors in the neocortex are both auto- and heteroreceptors, Neuroreport 7 (1996) 2773–2776.
[18] M.D. Ehlers, A.L. Mammen, L.-F. Lau, R.L. Huganir, Synaptic targeting of glutamate receptors, Curr. Opin. Cell Biol. 8 (1996) 484–489.
[19] J.C. Fiala, M. Feinberg, V. Popov, K.M. Harris, Synaptogenesis via dendritic filopodia in developing hippocampal area CA1, J. Neurosci. 18 (1998) 8900–8912.
[20] M. Glitsch, A. Marty, Presynaptic effects of NMDA in cerebellar Purkinje cells and interneurons, J. Neurosci. 19 (1999) 511–519.
[21] S. Halpain, A. Hipolito, L. Saffer, Regulation of F-actin stability in dendritic spines by glutamate receptors and calcineurin, J. Neurosci. 18 (1998) 9835–9844.
[22] G.W. Huntley, J.C. Vickers, W. Janssen, N. Brose, S.F. Heinemann, J.H. Morrison, Distribution and synaptic localization of immunocytochemically identified NMDA receptor subunit proteins in sensory-motor and visual cortices of monkey and human, J. Neurosci. 14 (1994) 3603–3619.
[23] L.C. Katz, C.J. Shatz, Synaptic activity and the construction of cortical circuits, Science 274 (2002) 1133.
[24] V.N. Kharazia, R.J. Weinberg, Immunogold localization of AMPA and NMDA receptors in somatic sensory cortex of albino rat, J. Comp. Neurol. 412 (1999) 292–302.
[25] U. Kistner, B.M. Wenzel, R.W. Veh, C. Cases-Langhoff, A.M. Barner, U. Appeltauer, B. Voss, E.D. Gundelfinger, C.C. Garner, SAP90, a rat presynaptic protein related to the product of the Drosophila tumor suppressor gene dlg-A, J. Biol. Chem. 268 (1993) 4580–4583.
[26] J.P. Kleinschmidt, Mechanisms of visual plasticity: Hebb synapses, NMDA receptors and beyond, Physiol. Rev. 71 (1991) 587–615.
[27] P. Koulen, E.L. Fletcher, S.E. Craven, D.S. Bredt, H. Wassle, Immunocytochemical localization of the postsynaptic density protein PSD-95 in the mammalian retina, J. Neurosci. 18 (1998) 10136–10149.
[28] J. Lehmann, R. Valentino, V. Robine, Cortical norepinephrine release elicited in situ by *N*-methyl-D-aspartate (NMDA) receptor stimulation: a microdialysis study, Brain Res. 599 (1992) 171–174.
[29] A. Luthi, L. Schwyzer, J.M. Mateos, B.H. Gahwiler, R.A. McKinney, NMDA receptor activation limits the number of synaptic connections during hippocampal development, Nat. Neurosci. 11 (2001) 1102–1107.
[30] R.A. McKinney, A. Luthi, C.E. Bandtlow, B.H. Gahwiler, S.M. Thompson, Selective glutamate receptor antagonists can induce or prevent axonal sprouting in rat hippocampal slice cultures, Proc. Natl. Acad. Sci. USA 96 (1999) 11631–11636.
[31] K.R. Melia, A. Trembleau, R. Oddi, P.P. Sanna, F.E. Bloom, Detection and regulation of tyrosine hydroxylase mRNA in catecholaminergic terminal fields: possible axonal compartmentalization, Exp. Neurol. 130 (1994) 394–406.
[32] B.M. Muller, U. Kistner, R.W. Veh, C. Cases-Langhoff, B. Becker, E.D. Gundelfinger, C.C. Garner, Molecular characterization and spatial distribution of SAP97, a novel presynaptic protein homologous to SAP90 and the *Drosophila* discs-large tumor suppressor protein, J. Neurosci. 15 (1995) 2354–2366.
[33] V.N. Murthy, T.J. Sejnowski, C.F. Stevens, Dynamics of dendritic calcium transients evoked by quantal release at excitatory hippocampal synapses, Proc. Natl. Acad. Sci. USA 97 (2000) 901–906.
[34] G. Nase, J. Weishaupt, P. Stern, W. Singer, H. Monyer, Genetic and epigenetic regulation of NMDA receptor expression in the rat visual cortex, Eur. J. Neurosci. 11 (1999) 4320–4326.
[35] M. Niethammer, E. Kim, M. Sheng, Interaction between the C terminus of NMDA receptor subunits and multiple members of the PSD-95 family of membrane-associated guanylate kinases, J. Neurosci. 16 (1996) 2157–2163.

[36] R.J. O'Brien, A.L. Mammen, S. Blackshaw, M.D. Ehlers, J.D. Rothstein, R.L. Huganir, The development of excitatory synapses in cultured spinal neurons, J. Neurosci. 17 (1997) 7339–7350.
[37] R.J. O'Brien, S. Kamboj, M.D. Ehlers, K.R. Rosen, G.D. Fischbach, R.L. Huganir, Activity-dependent modulation of synaptic AMPA receptor accumulation, Neuron 21 (1998) 1067–1078.
[38] S.A. Petersen, R.D. Fetter, J.N. Noordemeer, C.S. Goodman, Genetic analysis of glutamate receptors in Drosophila reveals a retrograde signal regulating presynaptic transmitter release, Neuron 19 (1997) 1237–1248.
[39] R.S. Petralia, Y.-X. Wang, R.J. Wenthold, The NMDA receptor subunits NR2A and NR2B show histological and ultrastructural localization patterns similar to those of NR1, J. Neurosci. 14 (1994) 6102–6120.
[40] R.S. Petralia, J.A. Esteban, Y.-X. Wang, J.G. Partridge, H.M. Zhao, R.J. Wenthold, Selective acquisition of AMPA receptors over postnatal development suggests a molecular basis for silent synapses, Nat. Neurosci. 2 (1999) 31–36.
[41] K.D. Phend, A. Rustioni, R.J. Weinberg, An osmium-free method of Epon embedment that preserves both ultrastructure and antigenicity for post-embedding immunocytochemistry, J. Histochem. Cytochem. 43 (1995) 283–292.
[42] J.P. Pierce, K. van Leyden, J.B. McCarthy, Translocation machinery for synthesis of integral membrane and secretory proteins in dendritic spines, Nat. Neurosci. 3 (2000) 311–313.
[43] E.M. Quinlan, B.D. Pohilpot, R.L. Huganir, M.F. Bear, Rapid, experience-dependent expression of synaptic NMDA receptors in visual cortex in vivo, Nat. Neurosci. 2 (1999) 352–357.
[44] I. Rajan, H.T. Cline, Glutamate receptor activity is required for normal development of tectal cell dendrites in vivo, J. Neurosci. 18 (1998) 7836–7846.
[45] I. Rajan, S. Witte, H.T. Cline, NMDA receptor activity stabilizes presynaptic retinotectal axons and postsynaptic optic tectal cell dendrites in vivo, J. Neurobiol. 38 (1999) 357–368.
[46] A. Rao, A.M. Craig, Activity regulates the synaptic localization of the NMDA receptor in hippocampal neurons, Neuron 19 (1997) 801–812.
[47] A. Rao, E. Kim, M. Sheng, A.M. Craig, Heterogeneity in the molecular composition of excitatory postsynaptic sites during development of hippocampal neurons in culture, J. Neurosci. 18 (1998) 1217–1229.
[48] J.R. Sanes, J.W. Lichtman, Induction, assembly, maturation and maintenance of a postsynaptic apparatus, Nat. Rev. Neurosci. 2 (2001) 791–805.
[49] M. Segal, P. Andersen, Dendritic spines shaped by synaptic activity, Curr. Opin. Neurobiol. 10 (2000) 582–586.
[50] M. Sheng, PDZs and receptor/channel clustering: rounding up the latest suspects, Neuron 17 (1996) 575–578, comment.
[51] O. Steward, mRNA localization in neurons: a multipurpose mechanism?, Neuron 18 (1997) 9–12.
[52] E. Veznedaroglu, T.A. Milner, Elimination of artifactual labeling of hippocampal mossy fibers seen following pre-embedding immunogold-silver technique by pretreatment with zinc chelator, Microsc. Res. Tech. 23 (1992) 100–101.
[53] J.M. Williams, S.E. Mason-Parker, W.C. Abraham, W.P. Tate, Biphasic changes in the levels of NMDAR-2 subunits correlate with the induction and persistence of LTP, Mol. Brain Res. 60 (1998) 21–27.
[54] G. Woodhall, D.I. Evans, M.O. Cunningham, R.S.G. Jones, NR2B-containing NMDA autoreceptors at synapses on entorhinal cortical neurons, J. Neurophysiol. 86 (2001) 1644–1651.
[55] R. Yuste, W. Denk, Dendritic spines as basic functional units of neuronal integration, Nature 375 (1995) 682–684.
[56] R. Yuste, A. Majewska, S.S. Cash, W. Denk, Mechanisms of calcium influx into hippocampal spines: heterogeneity among spines, coincidence detection by NMDA receptors and optical quantal analysis, J. Neurosci. 19 (1999) 1976–1987.
[57] N.E. Ziv, S.J. Smith, Evidence for a role of dendritic filopodia in synaptogenesis and spine formation, Neuron 17 (1996) 91–102.